Hindawi
Advances in Materials Science and Engineering
Volume 2020, Article ID 3685619, 17 pages
https://doi.org/10.1155/2020/3685619

Research Article

Test on Compaction Reinforcement Effect of Sand

Lianzhen Zhang,[1] Qingsong Zhang,[2] Zhipeng Li,[3] and Hongbo Wang[4]

[1]*College of Pipeline and Civil Engineering, China University of Petroleum, 66# Changjiang West Road, Qingdao, China*
[2]*Geotechnical and Structural Engineering Research Center, Shandong University, 17923# Jingshi Road, Jinan, China*
[3]*School of Transportation and Civil Engineering, Shandong Jiaotong University, Jinan, China*
[4]*Shandong Provincial Key Laboratory of Civil Engineering Disaster Prevention, Shandong University of Science and Technology, Qingdao, China*

Correspondence should be addressed to Qingsong Zhang; zhangqingsong@sdu.edu.cn

Received 16 March 2020; Revised 3 October 2020; Accepted 19 October 2020; Published 28 October 2020

Academic Editor: Lingxue Kong

In fracture or compaction grouting projects of sand layer, there exist many compacted sand regions on both sides of grout veins or around grout bulbs. It has an important effect on the final reinforcement effect of the sand layer that how much performance of the sand layer is improved after being compacted. Compression modulus, cohesion, and permeability coefficient are selected to be the performance indexes of the compaction reinforcement effect of sand. The relationship between the performance properties of sand and grouting pressure has been tested and analyzed. And influences of clay content and initial water ratio of sand on the compaction reinforcement effect have been studied. Results show that compaction can effectively improve the mechanical properties and impermeability properties of sand. Compression modulus of sand increases by 2~18 times. The cohesion of sand increases from the scope of 9.4~26 kPa to the scope of 40~113.6 kPa. The permeability coefficient of sand decreases from the scope of 1.0×10^{-2}~ 8.33×10^{-4} cm/s to the scope of 2.19×10^{-4}~2.77×10^{-9} cm/s. When the clay content of sand is smaller than about 20%, sand cannot be reinforced effectively by compaction. Cohesion cannot be improved significantly and the permeability coefficient cannot be reduced markedly. A high initial water ratio of sand is beneficial to improve the compression modulus of compacted sand and goes against the improvement of cohesion of compacted sand. In addition, the initial water ratio has little effect on the permeability coefficient of compacted sand. In the end, fitting formulas have been developed to quantitatively describe the compaction reinforcement effect of sand by different grouting pressures.

1. Introduction

Water-rich sand layer is characterized by rich water, low cementation strength, and low self-stability. When tunneling or digging foundation pit in water-rich sand layer, disaster accidents are likely to happen, such as collapse or sand inrush in tunnel or foundation pit [1–3]. The grouting method is widely used in underground engineering to reinforce the sand layer [4–7]. Many fracture or compaction grouting projects in the sand layer indicate that there exist many compacted sand regions on both sides of grout veins or around grout bulbs, as shown in Figure 1. Mechanical properties and impermeability of the sand layer will be improved after being compacted. Furthermore, the macroscopic performance of the sand layer improves under the combined reinforcement effect of grout veins, grout bulbs, and compacted sand. Consequently, it has a very important effect on the final reinforcement effect of the sand layer that how much performance of the sand layer is improved after being compacted.

Much research has been done to study the grouting mechanism of sand. Hyodo et al. [8–10] studied basic mechanical properties of sand under different load mode and drainage conditions. Considering filtration phenomena or time-dependent behavior of grout viscosity, Saada et al. [11], Yoon and El Mohtar [12], Axelsson et al. [13], Zhang [14], and Kim et al. [15] studied the permeation grouting process and established a series of theoretical models and

calculation methods. Bezuijen et al. [16] studied the fracture grouting process in sand and established an analytical model by simplifying the complicated shape of a fracture in sand into a geometrical shape. The width to length ratio of the fracture can be acquired eventually. In aspects of the grouting reinforcement effect of sand, Li et al. [17] measured performance parameters of the grouted body of sand under different water–cement ratios of cement slurry and curing time through a laboratory test. And two different destruction patterns for the grouted body in the uniaxial compression process were revealed, which are global destruction pattern at low W/C ratio and local destruction pattern at high W/C ratio. Yang et al. [18] analyzed influences of grouting pressure, grouting time, water–cement ratio, permeability coefficient, porosity upon grout diffusion radius, concretion strength, and their correlation, by grouting simulation test in sandy gravels. Qian et al. [19] took the model experiment method to study the permeability coefficient, porosity, and compressive strength of the porous medium before and after grouting operation with different effective diameters and fineness modulus. And permeability reduction law of chemical slurry for weakly porous media has been realized. Zhang et al. [20] put up a method to calculate the reinforcement effect of fracture-compaction grouting mode in soft strata. The research above is important for the study of grouting in the sand layer. However, most of them are concentrated on grouting diffusion and the reinforcement effect of sand with permeation mode. Little research has been done to realize the compaction reinforcement effect of sand. As a result, in fracture or compaction grouting projects of the sand layer, the reinforcement effect of grouted sand cannot be estimated accurately.

In this paper, the compaction reinforcement effect of sand has been studied. Clayey sand in Qingdao city of China is selected to be the typical sand material. Compression modulus, cohesion, and permeability coefficient are selected to be the performance indexes of the compaction reinforcement effect. Correspondingly, the consolidation test, consolidated-drained shear test, and falling head permeability test have been conducted to acquire the above performance indexes of sand at different compaction degrees. The relationship between the performance properties of sand and grouting pressure has been established. Subsequently, the influences of clay content and initial water ratio on the compaction reinforcement effect have been studied. In the end, fitting formulas have been developed to quantitatively describe the compaction reinforcement effect of sand by different grouting pressures.

2. Mechanism of Compaction Reinforcement of Sand

In the fracture or compaction grouting process, sand is compacted under grouting pressure. Correspondingly, the mechanical properties and impermeability of sand are improved in the following aspects as shown in Figure 2:

(1) Antideformation capacity of sand is improved after being compacted. Antideformation capacity of sand can be characterized by compression modulus. With compaction degree increasing, compaction of sand becomes more difficult and compression modulus of sand is improved correspondingly.

(2) Antidestruction capacity of sand is improved after being compacted. Destruction of sand normally appears in shear failure. Antidestruction capacity of sand can be characterized by shear strength parameters. Due to the low-stress level in stratum around digging face in underground engineering projects, whether shear failure occurs mainly depends on the cohesion of stratum. In this paper, the cohesion of sand is selected to represent the antidestruction capacity of sand. With compaction degree increasing, cementation between sand particles becomes stronger and cohesion of sand is improved correspondingly.

(3) Impermeability of sand is improved after being compacted. With compaction degree increasing, pore ratio and pore size between sand particles become smaller and the permeability coefficient decreases correspondingly.

Improvement of sand performance after being compacted is attributed to compression of voids and improvement of cementation capacity between sand particles. In this paper, clay content and initial water ratio of sand are selected as internal factors affecting the compaction reinforcement effect of sand. Grouting pressure is the power to compact sand, so that grouting pressure is selected as an external factor affecting the compaction reinforcement effect of sand.

3. Test Materials and Methods

Compression modulus, cohesion, and permeability coefficient are selected to be the performance indexes of the compaction reinforcement effect. Performance indexes of sand at different compaction degrees have been tested with different clay content and initial water ratio.

3.1. Test Materials. Clayey sand in Qingdao city of China is selected as the typical sand material, as shown in Figure 3, with water ratio of 20.2%, clay content (particle size smaller than 0.075 mm) of 14.91%, control grain size d_{60} of 1.75 mm, effective grain size d_{10} of 0.043 mm and d_{30} of 0.45 mm, coefficient of nonuniformity C_u of 40.7, and coefficient of curvature C_c of 2.69. The properties of clayey sand are shown in Table 1. The particle size distribution of clayey sand in Qingdao is shown in Figure 4. Clay components in the above sand are low liquid limit clay with liquid limit ω_l of 32% and plastic limit ω_p of 14%.

With the aim of studying the influences of clay content and initial water ratio on the compaction reinforcement effect of sand, remolded sand samples are manufactured by adjusting clay content and initial water ratio based on Qingdao clayey sand. Ten samples were used in the test. In order to study the influence of clay content on the compaction reinforcement effect, six samples (samples 1~6) are

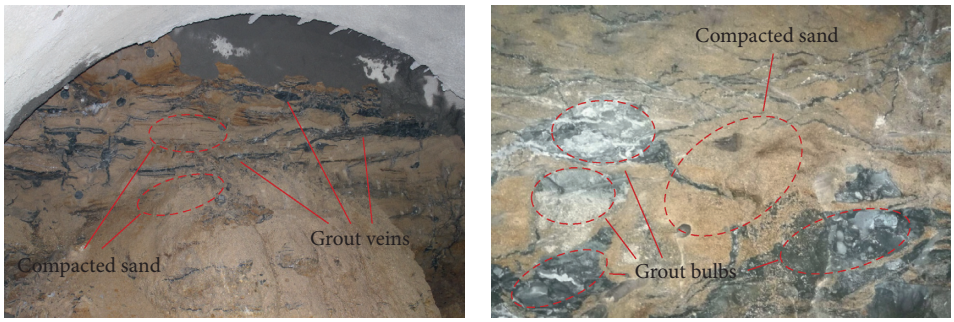

Figure 1: Photos of the grouted body in the sand. (a) Fracture grouting. (b) Compaction grouting.

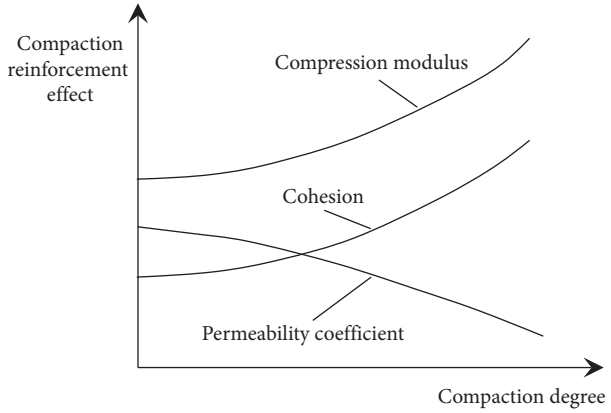

Figure 2: Relations of compaction reinforcement effect and compaction degree.

Figure 3: Photo of clayey sand in Qingdao.

designed with identical initial water ratio of 20% and different clay contents varying from 10% to 100%. In Table 2, 50% clay content is added, although 50% clay content means that the material used in this paper will be fine-grained soil not coarse-grained soil. Sample 6, with clay content of 100%, is pure clay and used for comparative analysis. In order to study the influence of the initial water ratio on the compaction reinforcement effect, five samples (sample 2 and samples 7~10) are designed with an identical clay content of 20% and different initial water ratios varying from 12% to 28%. The basic physical parameters of ten samples are shown in Table 2.

3.2. Test Methods

3.2.1. Compression Modulus. The consolidation test is used to acquire the relationship between pressure and strain in the compaction process with different sand samples. Due to a relatively good permeability of sand, drainage is allowed in the compaction process of sand in the consolidation test. According to engineering experiences of grouting projects, grouting pressure in sand is generally less than 2 MPa. Consequently, loading levels in the test are set at 50 kPa, 100 kPa, 200 kPa, 300 kPa, 500 kPa, 800 kPa, 1200 kPa, and 2000 kPa. When the deformation value per hour

corresponding to any loading level is lower than 0.005 mm, the compaction process is considered to be stable.

As shown in Figure 5, secant compression modulus in the consolidation test can be expressed as in the following equation [21]:

$$\overline{E}_s = \frac{p_{n+1} - p_n}{\varepsilon_{n+1} - \varepsilon_n}, \tag{1}$$

where ε_{n+1} and ε_n are strains corresponding to adjacent pressure p_{n+1} and p_n, respectively, and $\overline{E}_s$ is secant compression modulus.

In order to acquire a relationship between compression modulus and pressure equal to grouting pressure, tangent compression modulus at a pressure of $(p_{n+1} + p_n)/2$ is considered approximately equal to secant compression modulus corresponding to a pressure of p_{n+1} and p_n in this test. Tangent compression modulus at a pressure of $(p_{n+1} + p_n)/2$ can be expressed as

$$E_s|_{p=(p_{n+1}+p_n)/2} \approx \overline{E}_s = \frac{p_{n+1} - p_n}{\varepsilon_{n+1} - \varepsilon_n}. \tag{2}$$

The relationship between compression modulus and grouting pressure can be acquired after processing p-ε test data by equations (1) and (2).

3.2.2. Cohesion. The consolidated-drained shear test is used to acquire the shear strength of compacted sand. In this test, dry density of sand is used as a control index of compaction degree. Sand samples with different dry densities are tested to acquire shear strength at different compaction degrees. Sand samples are manufactured with dry densities of 1.45, 1.55, 1.65, 1.75, 1.85, 1.95, and 2.05 g/cm^3 for different clay content and initial water ratios. Clay content of sand samples is set at 10%, 20%, 30%, 40%, 50%, and 100% as shown in Table 2.

Different compaction stages of sand should be considered when setting the initial water ratio of sand samples. As shown in Figure 6, the compaction process of sand can be divided into two stages, nonsaturation stage and saturation stage. In the nonsaturation stage, the water ratio is constant and equal to the initial water ratio, with dry density increasing. Meanwhile, saturability increases with dry density increasing. When dry density exceeds a certain value, the nonsaturation stage inverts into the saturation stage and saturability is always equal to 1. In the saturation stage, the water ratio is lower than the initial water ratio and decreases with dry density increasing. It indicates that two sand samples with different initial water ratios will have the same water ratio when dry density exceeds a certain value. Under this condition, only one sand sample is needed to test and shear strength of sand samples with different initial water ratios can be acquired. Initial water ratio of sand samples is set at 12%, 16%, 20%, 24%, and 28% as shown in Table 2.

Logical connections between grouting pressure p, strain ε, pore ratio e, dry density ρ_d, and compaction reinforcement effect of sand are shown in Figure 7. The relationship between grouting pressure p and strain ε can be acquired by the consolidation test in this paper. The relationship between strain and pore ratio can be acquired by equation (3) [21]. The relationship between dry density ρ_d and pore ratio e satisfies equation (4) [21]. The relationship between cohesion c and dry density ρ_d can be acquired by the consolidated-drained shear test in this paper. Based on the above logical connections, the quantitative relationship between cohesion of sand and grouting pressure can be established eventually:

$$e = e_0 - (1 + e_0)\varepsilon, \tag{3}$$

where e is the pore ratio corresponding to strain ε and e_0 is the initial pore ratio:

$$e = \frac{\rho_s}{\rho_d} - 1, \tag{4}$$

where e is pore ratio of sand, ρ_s is grain density of sand, and ρ_d is dry density of sand.

3.2.3. Permeability Coefficient. Falling head permeability test is used to measure the permeability coefficient of compacted sand samples with different clay contents and compaction degrees. The reasons for using the falling head permeability test are as follows: firstly, the compaction degree of partial sand samples in this paper is relatively high, which results in the permeability being relatively low. The falling head permeability test method can measure the low permeability coefficient. And the constant head permeability test is not very applicable. Secondly, it is best to use only one kind of permeability test method to maintain the consistency of test results. Therefore, the falling head permeability test method is used in this paper. Due to the fact that sand sample is always saturated in the permeability test, the water ratio of sand is not considered in the permeability test operation. The effect of the initial water ratio on the permeability of sand is originated from its effect on the compaction process.

Similar to the test of sand cohesion, dry density of sand is used as a control index of compaction degree. Sand samples with different dry densities are tested to acquire the permeability coefficient at different compaction degrees. Dry density scope (1.45–2.05 g/cm^3) is the same as the test of sand cohesion. Moreover, the relationship between grouting pressure p, strain ε, pore ratio e, and dry density ρ_d can be acquired as shown in Figure 7. The relationship between permeability coefficient k and dry density ρ_d can be acquired by the permeability test in this paper. Eventually, the quantitative relationship between the permeability coefficient of sand and grouting pressure can be established.

4. Analysis of Test Results

4.1. Compression Modulus. Variation of the strain of sand with pressure under different conditions is shown in Figure 8. Clay content and initial water ratio of sand are denoted by q and ω_0, respectively:

(1) Strain increases nonlinearly with pressure in the compaction process of sand. Strain increases faster in

Table 1: Properties of clayey sand.

Water ratio (%)	Clay content (%)	d_{60} (mm)	d_{10} (mm)	d_{30} (mm)	Coefficient of nonuniformity, C_u	Coefficient of curvature, C_c
20.2	14.91	1.75	0.043	0.45	40.7	2.69

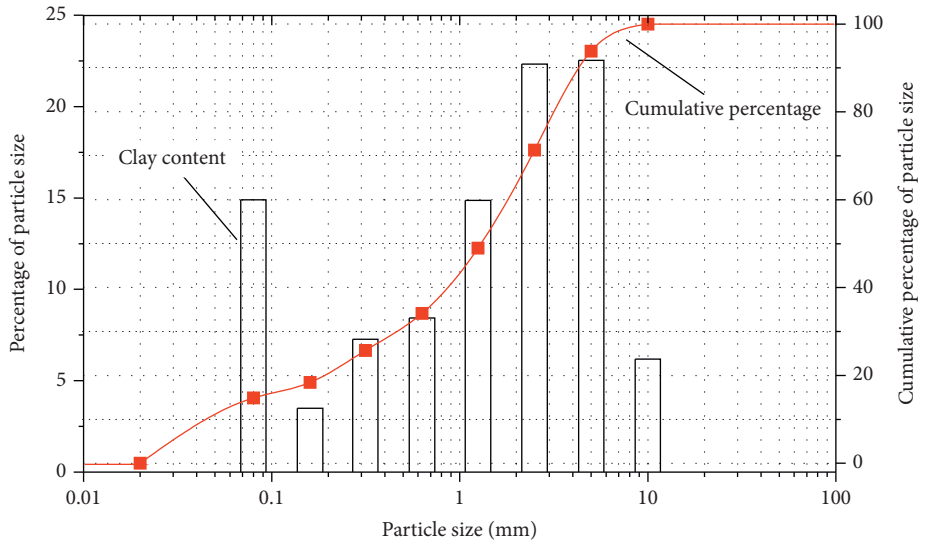

Figure 4: Particle size distribution of clayey sand in Qingdao.

Table 2: Basic physical parameters of sand samples.

Number	Clay content (%)	Initial water ratio, ω_0 (%)	Initial dry density, ρ_d	Grain specific gravity, G_s	Initial pore ratio, e_0	Initial saturability, S_r (%)
1	10	20	1.45	2.66	0.83	63.85
2	20	20	1.45	2.66	0.84	63.64
3	30	20	1.45	2.67	0.84	63.44
4	40	20	1.45	2.68	0.85	63.24
5	50	20	1.45	2.69	0.85	63.05
6	100	20	1.45	2.72	0.88	62.11
7	20	12	1.45	2.66	0.84	38.18
8	20	16	1.45	2.66	0.84	52.50
9	20	24	1.45	2.66	0.84	76.37
10	20	28	1.45	2.66	0.84	89.09

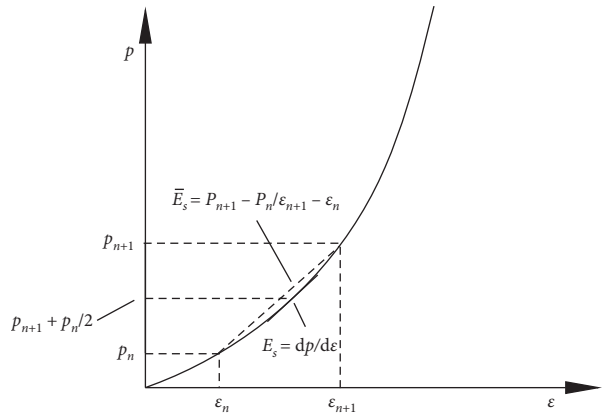

Figure 5: Sketch of secant and tangent compression modulus.

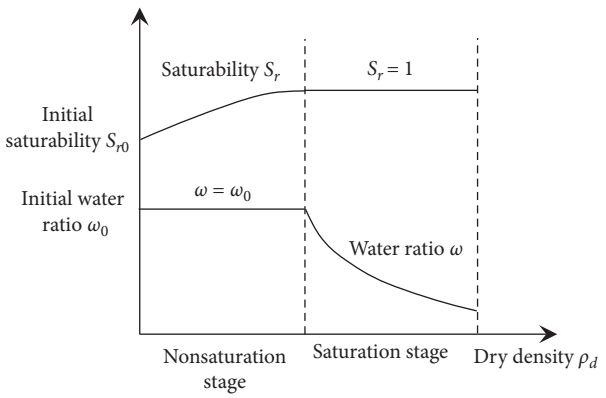

Figure 6: Variation of water ratio ω and saturability S_r during the compaction process.

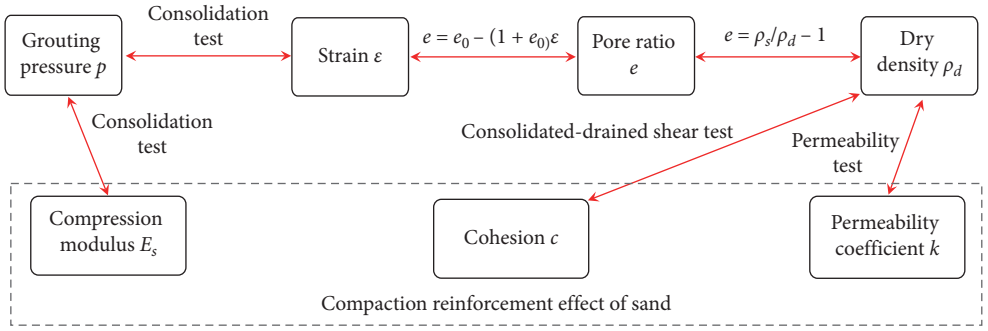

Figure 7: Logical connections between physical parameters.

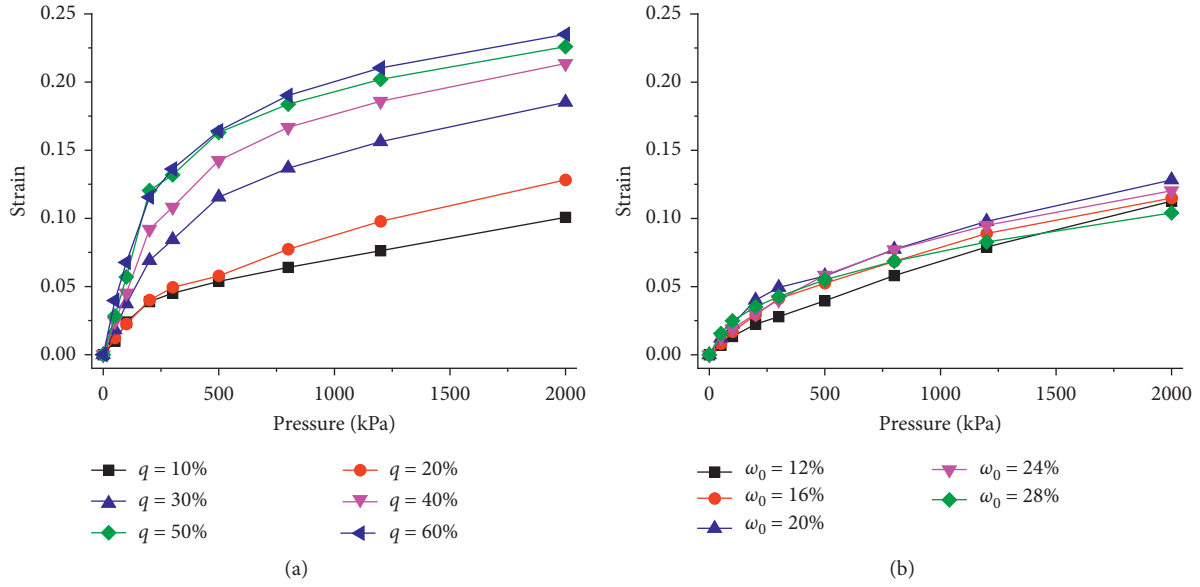

Figure 8: Variation of strain with pressure. (a) At different clay contents. (b) At different initial water ratios.

low-pressure scope than in high-pressure scope. And more than half of total deformation is accomplished with pressure increasing from 0 kPa to 500 kPa. With sand with clay content of 10%, total deformation is 0.101 at pressure of 2 MPa and deformation is 0.054 at pressure of 500 kPa which is more than half of 0.101. Difficulty to compact sand is growing during compaction process of sand.

(2) Clay content significantly affects the compaction process of sand. With clay content increasing, a higher strain value of sand at identical pressure is acquired. When clay content increases from 10% to 50%, the final strain of sand increases from 0.1 to 0.23 with an increasing rate of 130%. Sand can be considered to be composed of clay component (grain size smaller than 0.075 mm) and sand particle component (grain size bigger than 0.075 mm). The compressive property of clay component is significantly stronger than that of sand particle component and macroscopic compressive property of sand is affected by a combination of two components. As a result, compaction of sand becomes easier with clay content increasing. The strain-pressure curve of sand with a clay content of 50% is very similar to that of pure clay (with a clay content of 100%), in which clay component plays a decisive role in the compaction process of sand.

(3) As shown in Figure 8(b), the initial water ratio can affect the compaction process of sand. However, the effect of the initial water ratio is weaker than that of clay content. The final strain of sand is in the scope of 0.1 to 0.13, which is obviously smaller than the scope of sand strain caused by variation of clay content. Compared to the initial water ratio, the clay content is the main control factor affecting the compaction process of sand. When the initial water ratio increases from 12% to 20%, sand strain increases. By contrast, when the initial water ratio increases from 20% to 28%, sand strain decreases. It implies that an optimum initial water ratio exists. Sand strain decreases with the initial water ratio increasing or decreasing from the optimum value, which may be caused by the double layer effect of clay. When the water ratio is low, the water film on the surface of clay particles is very thin. Relative displacement of clay particles should overcome relatively large interparticle resistance. With water ratio increasing, the lubrication effect of water film on relative displacement of clay particles gradually appears resulting in sand strain being positively related to the water ratio. However, when the water ratio exceeds the optimal water ratio, the lubrication effect of water film is not sensitive to the water ratio. Moreover, when the water ratio continues to increase, there exist more closed bubbles in clay which are isolated from the atmosphere. The closed bubbles are difficult to be completely driven away, which is not conducive to the compaction process of sand. Therefore, when the water ratio exceeds the optimal water ratio, sand strain decreases with water ratio increasing.

Processing p-ε test data by equations (1) and (2): the relationship between compression modulus and grouting pressure under different conditions is acquired as shown in Figure 9:

(1) Compression modulus of sand is positively related to grouting pressure. The initial compression modulus of sand varies from 1.3 to 6.9 MPa, and the final compression modulus at grouting pressure of 2 MPa reaches a scope of 23~38 MPa. Compression modulus increases by 2~18 times, indicating that compaction by grouting pressure can effectively improve antideformation capacity of sand.

(2) With different clay content, the compression modulus of sand increases in different modes. When clay content is less than or equal to 20%, the compression modulus of sand increases nonlinearly with grouting pressure. Due to low clay content, the compaction process of sand is controlled by sand particle which has good antideformation capacity. In the early stage of compaction (with grouting pressure smaller than 400 kPa), sand particle skeleton has formed and compression modulus increases fast consequently. In the late stage of compaction (with grouting pressure increasing from 400 kPa to 2000 kPa), sand particles dislocate to achieve a lower pore ratio. However, sand particle dislocation cannot effectively improve the compression modulus of sand; therefore, the increase of grouting pressure cannot effectively improve compression modulus of sand.

(3) When clay content is in the scope of 30%~50%, the compression modulus of sand increases approximately linearly with grouting pressure. Due to high clay content, the compaction process of sand is controlled by the clay component. In the early stage of compaction, clay has good compressibility resulting in the compression modulus of sand increasing slowly. By contrast, after the compaction degree of sand reaches a certain value, clay particles are getting closer and the compression modulus of sand increases quickly. Eventually, there is little space for compaction, compression modulus of sand gradually approaches that of clay minerals. In addition, the compression modulus of sand with a clay content of 50% is approximately equal to that of pure clay.

(4) As shown in Figure 9(b), the initial water ratio of sand is negatively correlated with the initial compression modulus of sand. On the other hand, the initial water ratio of sand is positively correlated with the final compression modulus of sand (except for $\omega_0 = 16\%$). In other words, greater improvement of the compression modulus of sand can be acquired with a higher initial water ratio.

4.2. Cohesion. Variation of cohesion of sand with pore ratio under different conditions is shown in Figure 10. The cohesion of sand increases nonlinearly during the reduction of pore ratio. In the compaction process, spacing between sand particles and clay particles becomes smaller resulting in cohesion increasing faster. With clay content of 10% and initial water ratio of 20%, the cohesion of sand increases

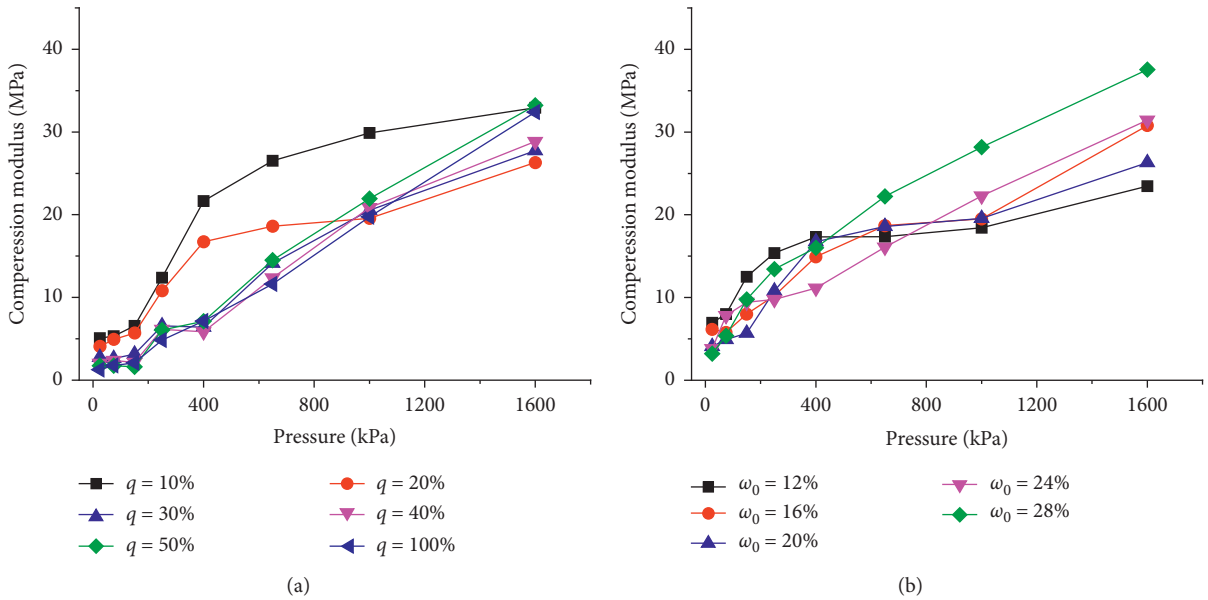

Figure 9: Relationship between compression modulus and grouting pressure. (a) At different clay contents. (b) At different initial water ratios.

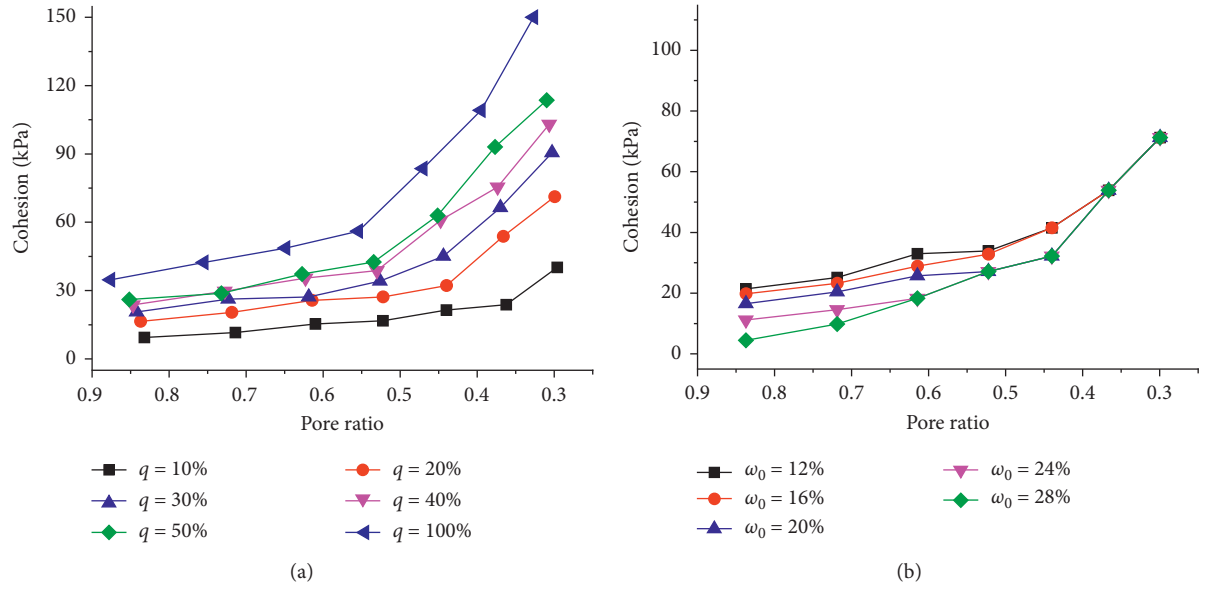

Figure 10: Variation of cohesion with pore ratio. (a) At different clay contents. (b) At different initial water ratios.

from 9.4 kPa to 40 kPa when the pore ratio decreases from 0.83 to 0.3. Meanwhile, with a clay content of 100% and an initial water ratio of 20%, cohesion of pure clay increases from 40 kPa to 150 kPa at the same variation of pore ratio. It is revealed that the shear strength of sand can be improved effectively by compaction.

Due to the fact that effective cohesive force between sand particles is difficult to form and clay component is the only source of macroscopic cohesion of sand, clay content has a significant effect on the cohesion of sand which is mainly reflected in the following two aspects:

(1) With clay content increasing, the initial cohesion of sand increases. When clay content increases from 10% to 100%, the initial cohesion of sand increases from 9.4 kPa to 34.7 kPa which is 3.7 times the initial value.

(2) With clay content increasing, the growth value of cohesion increases faster. At the same reduction of pore ratio, the growth value of cohesion with high clay content is higher than that with low clay content. When the pore ratio decreases from about 0.85 to

about 0.3, cohesion of sand with a clay content of 50% increases from 26.0 kPa to 113.6 kPa and cohesion of sand with a clay content of 10% merely increases from 9.4 kPa to 40.2 kPa.

As shown in Figure 10(b), the initial water ratio is negatively related to the cohesion of sand. An increase in the initial water ratio goes against the improvement of the shear strength of sand. In the compaction process of sand, cohesion increases with pore ratio decreasing and sand is unsaturated until the pore ratio is reduced to a certain value. With pore ratio continuously decreasing, sand with initial water ratio of 28% reaches saturated state first and sand with initial water ratio of 24% reaches saturated state subsequently. As a result, two sand samples with different initial water ratios are in identical physical state (with identical pore ratio, saturability, and water ratio), and two corresponding *c-e* curves merge into one identical curve. Furthermore, more *c-e* curves merge into one identical curve in the late compaction process. When the pore ratio of sand decreases to about 0.32, all five *c-e* curves merge into one curve.

The relationship between cohesion of sand and grouting pressure under different conditions is shown in Figure 11. When clay content is less than or equal to 20%, the cohesion of sand increases not significantly and approximately linearly with grouting pressure. And clay content effectively influences the slope of *c-p* curves. Slope corresponding to clay content of 20% is higher than that when clay content equals 10%. When clay content is in the scope of 30%~50%, cohesion increases nonlinearly with grouting pressure. The cohesion of sand grows more slowly with grouting pressure increasing. In general, the cohesion of sand with different clay content is obviously lower than the cohesion of pure clay at identical grouting pressure. As shown in Figure 11(b), the initial water ratio has little effect on the cohesion of sand. When the initial water ratio varies from 12% to 28%, the growth value of cohesion is always about 17 kPa at any grouting pressure and the slope of *c-p* curves changes little. However, the intercept of *c-p* curves increases with the initial water ratio decreasing.

4.3. Permeability Coefficient. Variation of the permeability coefficient of sand with pore ratio under different conditions is shown in Figure 12, with the permeability coefficient represented in logarithmic form:

(1) Permeability coefficient of sand decreases with pore ratio decreasing. When the pore ratio decreases from 0.87 to 0.3, the permeability coefficient decreases by 2 to 5 orders of magnitude with different clay contents. It is revealed that the impermeability of sand can be improved effectively by compaction.

(2) lg (k) is approximately linearly related to pore ratio e, which indicates that the permeability coefficient decreases nonlinearly with the reduction of pore ratio. The reduction of pore ratio would accelerate the decrease of the permeability coefficient. Clay content has a significant effect on the permeability coefficient of sand which is mainly reflected in the following two aspects. (1) Initial permeability coefficient decreases with clay content increasing. Initial permeability coefficient corresponding to clay content of $q = 10\%$ and $q = 100\%$ is 1.0×10^{-2} cm/s and 2.19×10^{-4} cm/s, respectively, with a difference of two orders of magnitude. (2) The permeability coefficient of sand is more sensitive with compaction when clay content is higher. In other words, the magnitude of reduction of permeability coefficient at an identical reduction of pore ratio is higher if clay content is higher. When the pore ratio decreases from 0.87 to 0.3, the reduction of permeability coefficient corresponding to clay content of $q = 10\%$ and $q = 100\%$ is $1.0 \times 10^{-2} \longrightarrow 2.21 \times 10^{-4}$ cm/s (decreasing by 2 orders of magnitude) and $2.19 \times 10^{-4} \longrightarrow 2.77 \times 10^{-9}$ cm/s (decreasing by 5 orders of magnitude), respectively. When clay content is less than or equal to 20%, the permeability of sand is controlled by a sand particle skeleton whose void size is relatively big and pore connectivity is relatively good. Consequently, the initial permeability coefficient is relatively high. In the compaction process of sand, the sand particle skeleton is compacted. However, there is no qualitative change of void size and pore connectivity, resulting in the permeability coefficient being relatively high at any pore ratio. When the clay content is in the scope of 30%~50%, the permeability coefficient of sand is controlled by the clay component. Due to the small particle size of clay component (smaller than 0.075 mm), the initial permeability coefficient of sand is relatively low. When the pore ratio reaches about 0.3, the permeability coefficient of compacted sand with a clay content of 50% is smaller than 2.77×10^{-9} cm/s with excellent impermeability.

The relationship between the permeability coefficient of sand and grouting pressure under different conditions is shown in Figure 13. lg (k) increases nonlinearly with grouting pressure. When grouting pressure is in low scope, an increase of grouting pressure would cause an evident reduction of permeability coefficient. By contrast, when grouting pressure is in high scope, the permeability coefficient is little sensitive with grouting pressure. Permeability coefficient decreases faster with the increase of grouting pressure when clay content is higher. In general, the permeability coefficient of sand with different clay content is obviously higher than that of pure clay at identical grouting pressure.

The effect of the initial water ratio on the permeability coefficient of sand merely originated from its effect on the compaction process. The variation range of the finial sand strain at grouting pressure of 2 MPa is 0.1~0.13 which is a relatively small range, as shown in Figure 8(b), indicating that the initial water ratio has little effect on the compaction process of sand. As a result, the initial water ratio affects the

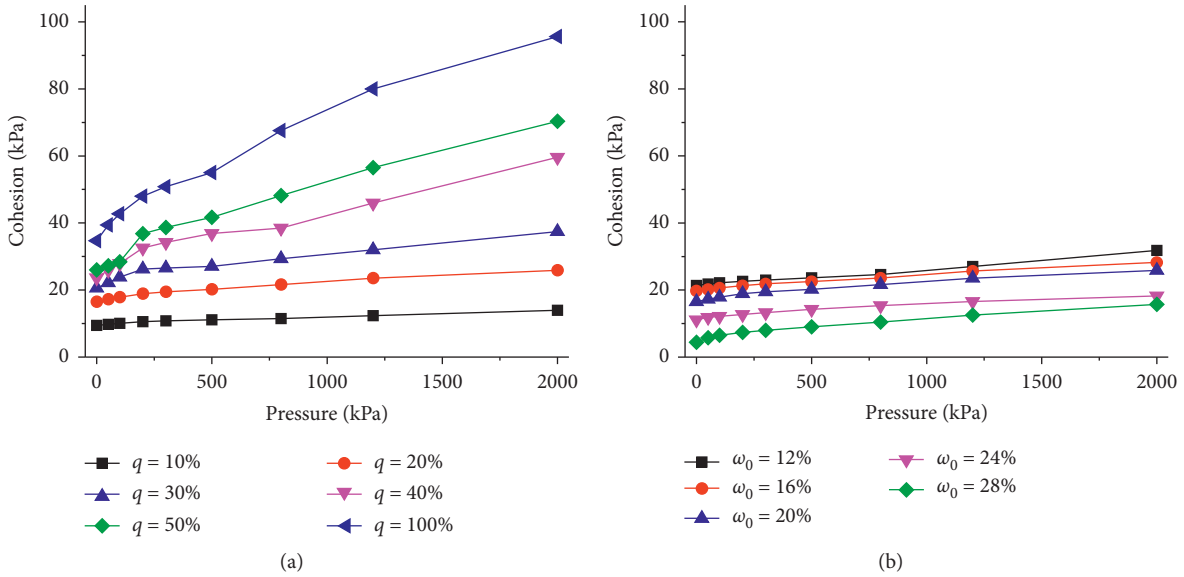

Figure 11: Relationship between cohesion of sand and grouting pressure. (a) At different clay contents. (b) At different initial water ratios.

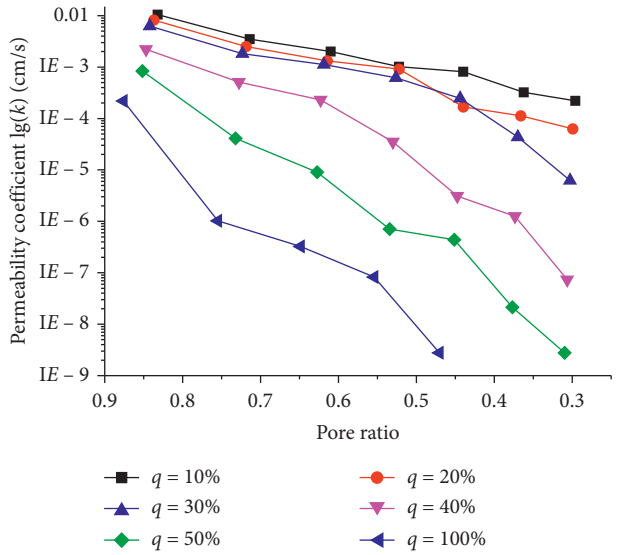

Figure 12: Relationship between permeability coefficient and pore ratio.

permeability coefficient slightly. In addition, due to the optimum initial water ratio of 20% in the compaction process of sand, the permeability coefficient with an initial water ratio of 20% has the lowest permeability coefficient at any grouting pressure.

5. Analysis of Applicability of Compaction Reinforcement Method

In this section, the applicability of the compaction reinforcement method for sand is analyzed in the aspect of self-characteristics of sand. For the convenience of analysis, the condition of grouting pressure of 2 MPa is selected as the typical condition. Comparison of performance indexes (compression modulus, cohesion, and permeability coefficient) before and after compaction is shown in Figures 14–16.

As shown in Figure 14, the initial compression modulus of sand is negatively related to clay content. With clay content increasing, the growth rate of the compression modulus increases fast. However, growth value (22~31 MPa) and finial compression modulus (26~33 MPa) vary little and maintain a high value. Therefore, the compression modulus of sand can be improved efficiently by compaction regardless of the clay content of sand. The initial compression modulus of sand is negatively related to the initial water ratio of sand.

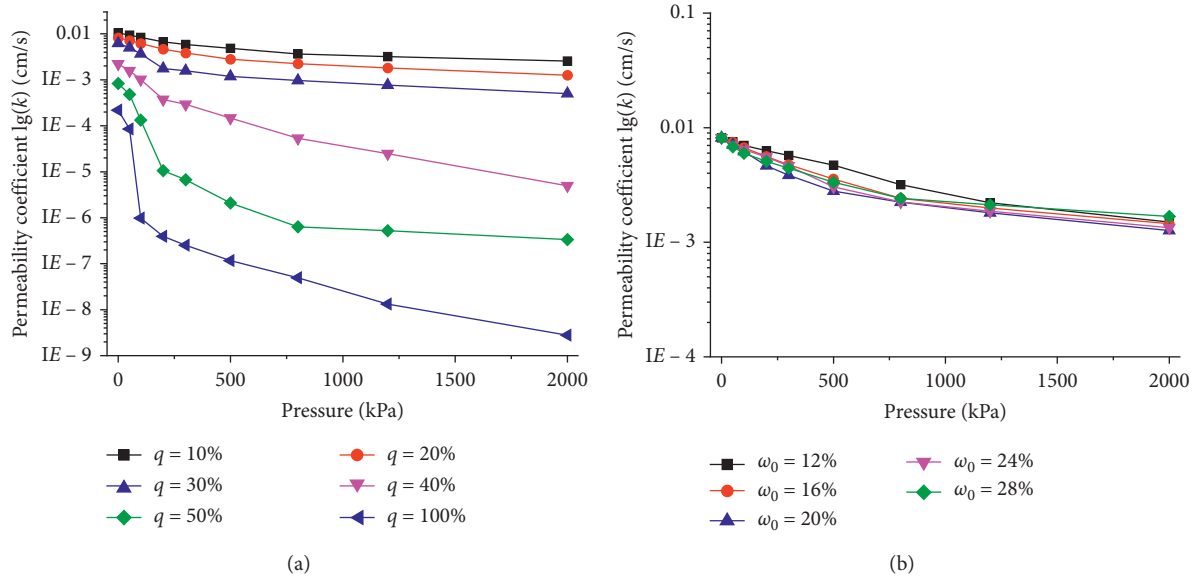

FIGURE 13: Relationship between permeability coefficient of sand and grouting pressure. (a) At different clay contents. (b) At different initial water ratios.

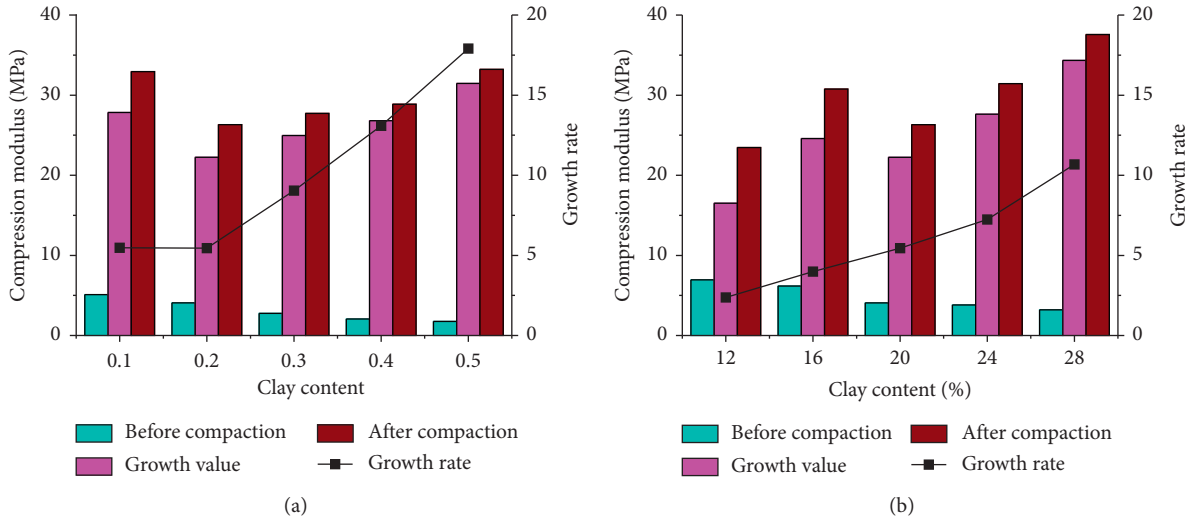

FIGURE 14: Comparison of compression modulus before and after compaction ($p = 2$ MPa). (a) At different clay contents. (b) At different initial water ratios.

By contrast, growth value, finial compression modulus, and growth rate are all positively related to the initial water ratio. When the initial water ratio increases from 12% to 28%, the growth rate of compression modulus increases from 2.4 to 10.7. Therefore, in view of the compression modulus, a high initial water ratio is beneficial to improve the compaction reinforcement effect of sand.

As shown in Figure 15, compacted by grouting pressure of 2 MPa, the initial value, growth value, and finial value of cohesion of sand all increase with clay content increasing. Correspondingly, the growth rate increases from 48.1% to 170.4%. When clay content is less than or equal to 20%, initial cohesion (<17 kPa) and growth value (<10 kPa) maintains a quite low level and the growth rate of cohesion of sand compacted by grouting pressure of 2 MPa is smaller than 57%. Shear strength of compacted sand is difficult to meet the engineering requirements of stability. It indicates that the cohesion of sand with relatively low clay content cannot be improved effectively even though high grouting pressure is used in compaction. As shown in Figure 15(b), with the initial water ratio increasing, the initial value and finial value of cohesion of sand decrease at the same time. However, the growth value of cohesion is basically unchanged at any initial water ratio and the growth rate

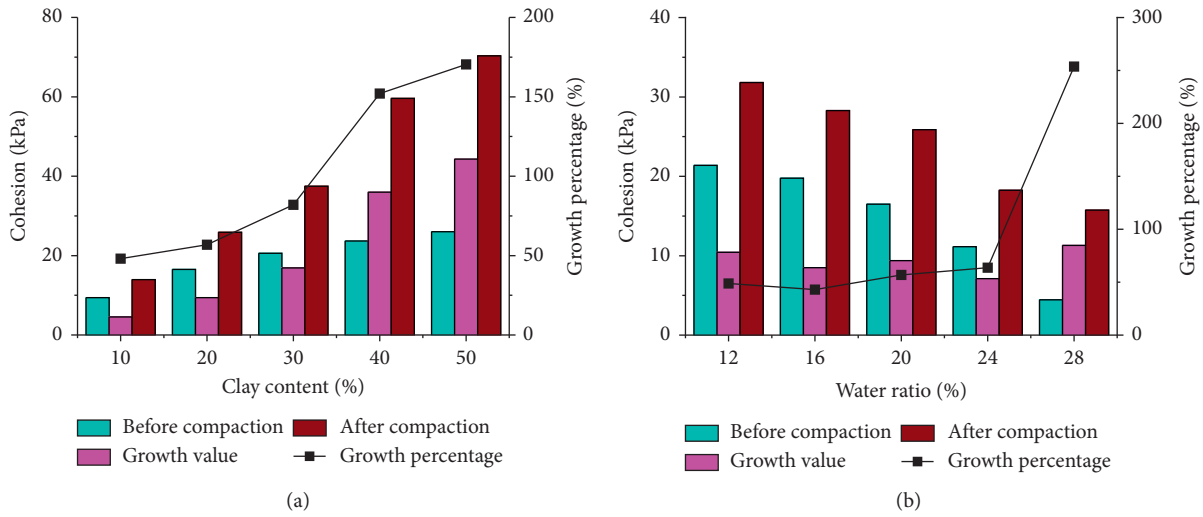

Figure 15: Comparison of cohesion before and after compaction ($p = 2$ MPa). (a) At different clay contents. (b) At different initial water ratios.

increases due to the reduction of the initial value. In general, in view of cohesion, a high initial water ratio goes against the improvement of the compaction reinforcement effect of sand.

As shown in Figure 16, compacted by grouting pressure of 2 MPa, the initial value and finial value of permeability coefficient are negatively related to clay content and reduction degree of permeability coefficient is positively related to clay content. When clay content increases from 10% to 50%, the reduction degree of permeability coefficient increases from 0.61 orders of magnitude to 3.39 orders of magnitude. When clay content is less than or equal to 20%, the initial permeability coefficient and finial value ($\geq 1.26 \times 10^{-3}$ cm/s) maintains a quite high level which is difficult to meet engineering requirements of impermeability. The reduction degree of permeability coefficient of sand compacted by grouting pressure of 2 MPa is smaller than one order of magnitude. It indicates that the impermeability of sand with relatively low clay content cannot be improved effectively even though high grouting pressure is used in compaction. As shown in Figure 16(b), the initial water ratio has little effect on the initial value, final value, or reduction degree of permeability coefficient of sand.

In general, when the clay content of sand is smaller than a certain value, cohesion cannot be improved effectively and the permeability coefficient cannot be reduced effectively. Meanwhile, the compression modulus of sand can be improved efficiently by compaction regardless of the clay content of sand. Consequently, when clay content is smaller than a certain value, sand cannot be reinforced effectively by compaction. On the other hand, high initial water ratio of sand is beneficial to improve the compression modulus of compacted sand and goes against the improvement of cohesion of compacted sand. In addition, the initial water ratio has little effect on the permeability coefficient of compacted sand. Therefore, the influence of the initial water ratio of sand on the compaction reinforcement effect is multifaceted and complicated.

6. Formula Fitting of Compaction Reinforcement Effect of Sand

6.1. Compression Modulus. With the objective to quantitatively describe the relationship between compression modulus of sand and grouting pressure considering different clay content and initial water ratio of sand, formulas fitting of E_s-p curves have been done. Based on the above analysis, there is a significant difference between E_s-p curves with clay contents of 10% and 20% and those with clay contents of 30% to 50%. On the other hand, the initial water ratio has little effect on the characteristics of E_s-p curves. When clay content of sand is less than or equal to 20%, logarithmic equation form, $y = A + B\ln(x + C)$, is used to fit E_s-p curves where y is compression modulus, x is grouting pressure, and A, B, and C are constants, respectively. When clay content of sand is in the scope of 30% to 50%, linear equation form, $y = Ax + B$, is used to fit E_s-p curves where y, x, A, and B have the same meaning as the above statement. Fitting equations of E_s-p curves and adjusted R Square are shown in Table 3. Partial fitting curves are shown in Figure 17. Adjusted R Square of fitting equations is all bigger than 0.93, indicating good fitting effect.

6.2. Cohesion. When the clay content of sand is less than or equal to 20%, the cohesion of sand increases approximately linearly with grouting pressure. Thus, a linear equation form, $y = Ax + B$, is used to fit c-p curves where y is cohesion, x is grouting pressure, and A and B are constants, respectively. When the clay content of sand is in the scope of 30% to 50%, the cohesion of sand increases nonlinearly with grouting pressure. The logarithmic equation form, $y = A + B\ln(x + C)$, is used to fit c-p curves. Fitting equations of c-p curves and adjusted R Square are shown in Table 4. Partial fitting curves are shown in Figure 18. Adjusted R Square of fitting

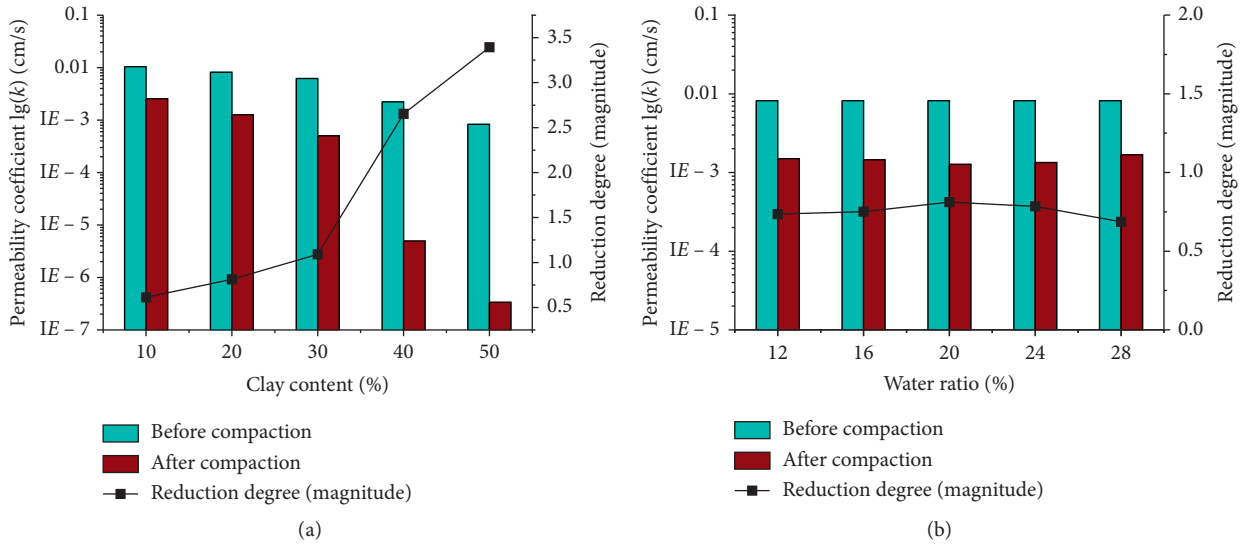

Figure 16: Comparison of permeability coefficient before and after compaction ($p = 2$ MPa). (a) At different clay contents. (b) At different initial water ratios.

Table 3: Fitting results of E_s-p curves.

Condition	Fitting equation	Adjusted R Square
$q = 10\%$, $\omega_0 = 20\%$	$E_s = -72.695 + 14.426 \ln(p + 162.85)$	$R^2 = 0.94$
$q = 20\%$, $\omega_0 = 20\%$	$E_s = -52.87 + 10.52 \ln(p + 177.76)$	$R^2 = 0.94$
$q = 30\%$, $\omega_0 = 20\%$	$E_s = 0.0171p + 1.6311$	$R^2 = 0.98$
$q = 40\%$, $\omega_0 = 20\%$	$E_s = 0.0181p + 0.6946$	$R^2 = 0.98$
$q = 50\%$, $\omega_0 = 20\%$	$E_s = 0.02p + 1.112$	$R^2 = 0.99$
$q = 20\%$, $\omega_0 = 12\%$	$E_s = -11.585 + 4.585 \ln(p + 26.429)$	$R^2 = 0.93$
$q = 20\%$, $\omega_0 = 16\%$	$E_s = -237.74 + 33.32 \ln(p + 1463.3)$	$R^2 = 0.96$
$q = 20\%$, $\omega_0 = 24\%$	$E_s = -2080.1 + 220.7 \ln(p + 12716.8)$	$R^2 = 0.98$
$q = 20\%$, $\omega_0 = 28\%$	$E_s = -146.7 + 24.01 \ln(p + 499.83)$	$R^2 = 0.99$

Where unit of E_s and p is MPa and kPa, respectively.

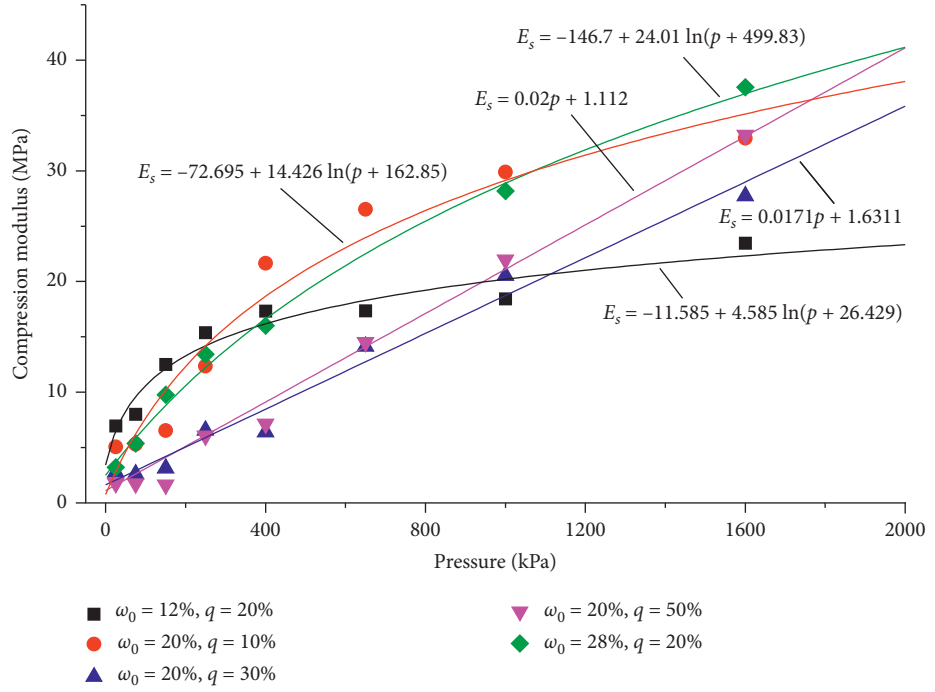

Figure 17: Fitting curves of compression modulus and pressure.

Table 4: Fitting results of c-p relation.

Condition	Fitting equation	Adjusted R Square
$q = 10\%$, $\omega_0 = 20\%$	$c = 0.0021p + 9.848$	$R^2 = 0.97$
$q = 20\%$, $\omega_0 = 20\%$	$c = 0.0045p + 17.547$	$R^2 = 0.96$
$q = 30\%$, $\omega_0 = 20\%$	$c = -49.32 + 10.89\ln(p + 682.11)$	$R^2 = 0.95$
$q = 40\%$, $\omega_0 = 20\%$	$c = -569.9 + 72.96\ln(p + 3521.36)$	$R^2 = 0.96$
$q = 50\%$, $\omega_0 = 20\%$	$c = -234.19 + 38.01\ln(p + 946.43)$	$R^2 = 0.98$
$q = 20\%$, $\omega_0 = 12\%$	$c = 0.005p + 21.387$	$R^2 = 0.99$
$q = 20\%$, $\omega_0 = 16\%$	$c = 0.0042p + 20.274$	$R^2 = 0.99$
$q = 20\%$, $\omega_0 = 24\%$	$c = 0.0035p + 11.964$	$R^2 = 0.95$
$q = 20\%$, $\omega_0 = 28\%$	$c = 0.0053p + 5.8724$	$R^2 = 0.96$

Where unit of c and p is kPa.

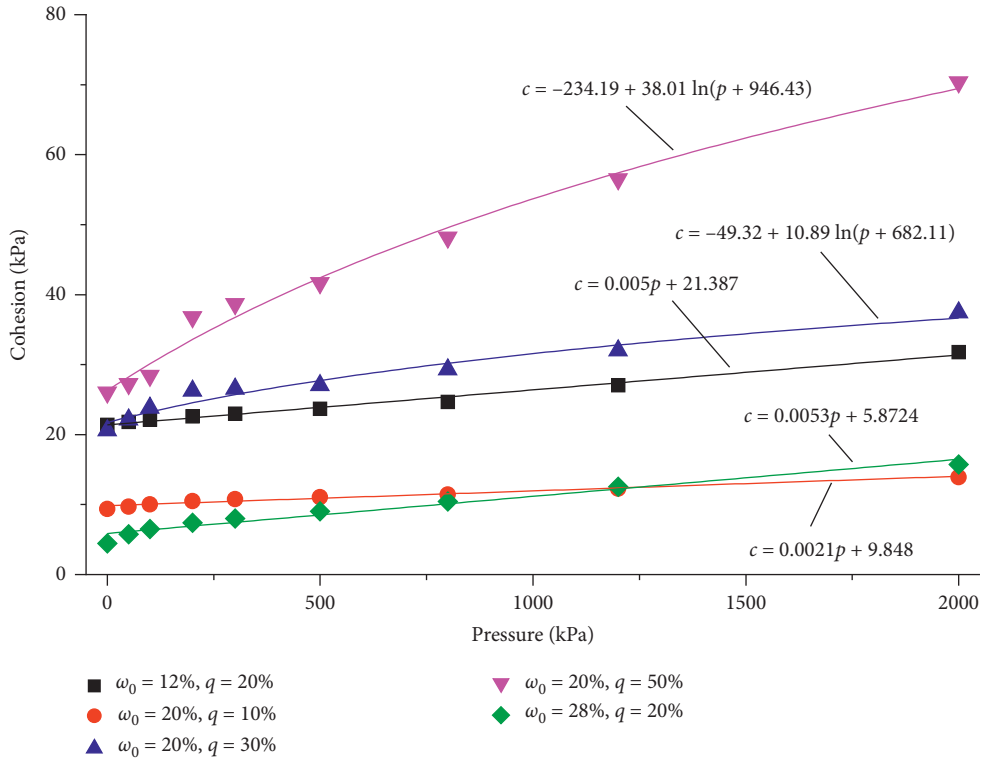

Figure 18: Fitting curves of cohesion and pressure.

Table 5: Fitting results of k-p relation.

Condition	Fitting equation	Adjusted R Square
$q = 10\%$, $\omega_0 = 20\%$	$k = 10^{-2.8+(564.3/(p+683.1))}$	$R^2 = 0.99$
$q = 20\%$, $\omega_0 = 20\%$	$k = 10^{-3.16+(737.51/(p+685.66))}$	$R^2 = 0.99$
$q = 30\%$, $\omega_0 = 20\%$	$k = 10^{-3.41+(385.11/(p+312.73))}$	$R^2 = 0.98$
$q = 40\%$, $\omega_0 = 20\%$	$k = 10^{-6.84+(5253.3/(p+1268.9))}$	$R^2 = 0.99$
$q = 50\%$, $\omega_0 = 20\%$	$k = 10^{-7.05+(1040.9/(p+249.9))}$	$R^2 = 0.98$
$q = 20\%$, $\omega_0 = 12\%$	$k = 10^{-3.9+(5146/(p+2827.6))}$	$R^2 = 0.99$
$q = 20\%$, $\omega_0 = 16\%$	$k = 10^{-3.25+(1237.58/(p+1050.1))}$	$R^2 = 0.99$
$q = 20\%$, $\omega_0 = 24\%$	$k = 10^{-3.26+(1106.1/(p+939.87))}$	$R^2 = 0.99$
$q = 20\%$, $\omega_0 = 28\%$	$k = 10^{-3.02+(641.77/(p+695.04))}$	$R^2 = 0.99$

Where unit of k and p is cm/s and kPa, respectively.

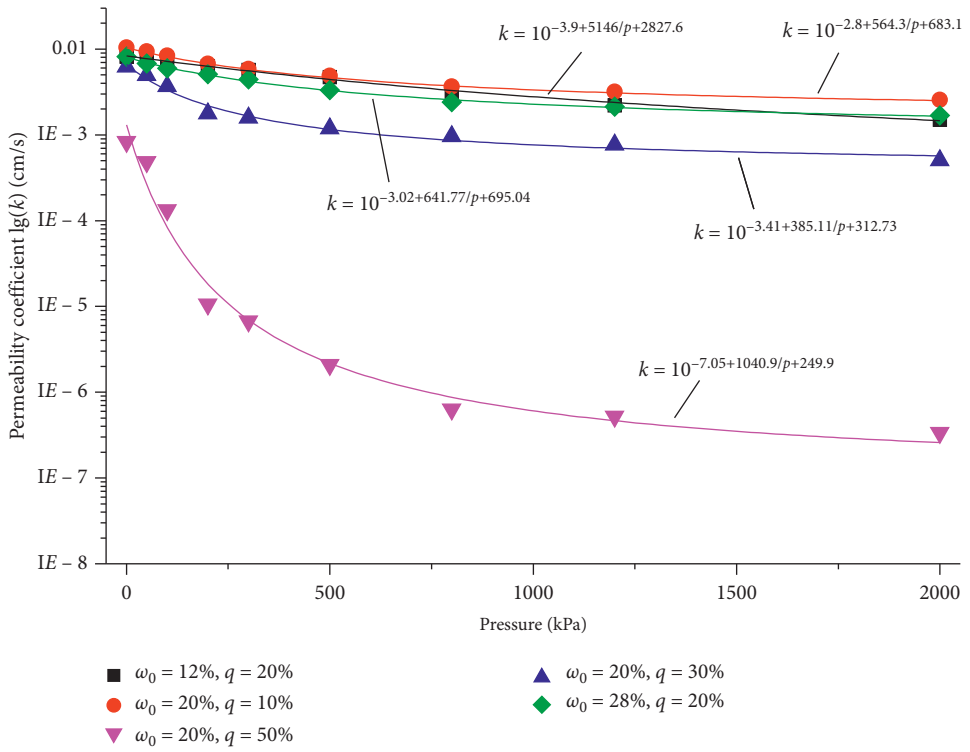

Figure 19: Fitting curves of permeability coefficient and pressure.

equations is all bigger than 0.95, indicating a good fitting effect.

6.3. Permeability Coefficient. Considering that lg (k) decreases nonlinearly with grouting pressure, the hyperbolic equation form, $y = Ax + B/(x + C)$, is used to fit lg (k)-p curves where y is lg (k), x is grouting pressure, and A, B, and C are constants, respectively. Fitting equations of lg (k)-p curves and adjusted R Square are shown in Table 5. Partial fitting curves are shown in Figure 19. Adjusted R Square of fitting equations is all bigger than 0.98, indicating good fitting effect.

In general, when the clay content of sand is less than or equal to 20%, the relationship between the compaction reinforcement effect of sand and grouting pressure can be quantitatively described by

$$\begin{cases} E_s = A_1 + B_1 \ln(p + C_1), \\ c = A_2 p + B_2, \\ k = 10^{A_3 + (B_3/(p + C_3))}, \end{cases} \quad (5)$$

where E_s, c, and k are compression modulus (unit: MPa), cohesion (unit: kPa), and permeability coefficient (unit: cm/s), respectively; p is grouting pressure (unit: kPa); and A_i, B_i, and C_i ($i = 1, 2, 3$) are constants determined by clay content and initial water ratio of sand.

When clay content of sand is in the scope of 30% to 50%, the relationship between the compaction reinforcement effect of sand and grouting pressure can be quantitatively described by

$$\begin{cases} E_s = D_1 p + E_1, \\ c = C_2 + D_2 \ln(p + E_2), \\ k = 10^{A_3 + (B_3/(p + C_3))}, \end{cases} \quad (6)$$

where A_i, B_i, C_i, D_i, and E_i ($i = 1, 2, 3$) are constants determined by clay content and initial water ratio of sand.

Applicable conditions of equations (5) and (6) are as follows: firstly, clay content of sand is in the scope of 10% to 50%. Secondly, the initial water ratio of sand is in the range of 12% to 28%. Thirdly, grouting pressure is less than or equal to 2 MPa. By equations (5) and (6), the mechanical properties and impermeability properties of sand compacted by specific grouting pressure can be calculated. When clay content or initial water ratio is an arbitrary value, the interpolation method can be used to determine the value of compression modulus E_s, cohesion c, and permeability coefficient k of sand. However, the physical meaning of the constants A, B, C, D, and E has not been fully studied. In future research, this problem should be studied comprehensively.

7. Conclusion

Mechanical properties and impermeability properties of sand at different compaction degrees are quantitatively tested and analyzed. And influences of clay content and initial water ratio on the compaction reinforcement effect have been studied. Conclusions are as follows.

(1) Compaction can effectively improve the mechanical properties and impermeability properties of sand.

Under the present experimental conditions in this paper, the compression modulus of sand increases by 2~18 times, from the scope of 1.3~6.9 MPa to the scope of 23~38 MPa. The cohesion of sand increases from the scope of 9.4~26 kPa to the scope of 40~113.6 kPa. The permeability coefficient of sand decreases from the scope of 1.0×10^{-2}~8.33×10^{-4} cm/s to the scope of 2.19×10^{-4}~2.77×10^{-9} cm/s.

(2) When clay content of sand is smaller than a certain value, cohesion cannot be improved effectively and the permeability coefficient cannot be reduced effectively. Meanwhile, the compression modulus of sand can be improved efficiently by compaction regardless of the clay content of sand. Consequently, when clay content is smaller than a certain value, sand cannot be reinforced effectively by compaction.

(3) High initial water ratio of sand is beneficial to improve the compression modulus of compacted sand and goes against the improvement of cohesion of compacted sand. In addition, the initial water ratio has little effect on the permeability coefficient of compacted sand. Therefore, the influence of the initial water ratio of sand on the compaction reinforcement effect is multifaceted and complicated.

(4) Quantitative fitting formulas under laboratory conditions have been obtained that can describe the relationship between compaction reinforcement effect of sand and grouting pressure, at different clay contents and initial water ratios. The compaction reinforcement effect of sand can be predicted using these fitting formulas.

Data Availability

The data used to support the findings of this study are available from the corresponding author upon request.

Conflicts of Interest

The authors declare that they have no conflicts of interest.

Acknowledgments

This work was supported by the National Key Research and Development Project (2018YFB1600200); the National Natural Science Foundation of China (Grant nos. 51909270 and 51909147); the Fundamental Research Funds for the Central Universities (Grant no. 18CX02003A); and the Natural Science Foundation of Shandong Province (Grant no. ZR2018BEE035).

References

[1] Y.-q. Wu, K. Wang, L.-z. Zhang, and S.-h. Peng, "Sand-layer collapse treatment: an engineering example from Qingdao Metro subway tunnel," *Journal of Cleaner Production*, vol. 197, pp. 19–24, 2018.

[2] D.-M. Zhang, Z.-K. Huang, R.-L. Wang, J.-Y. Yan, and J. Zhang, "Grouting-based treatment of tunnel settlement: practice in Shanghai," *Tunnelling and Underground Space Technology*, vol. 80, pp. 181–196, 2018.

[3] Y. Liang, W. Sui, and J. Qi, "Experimental investigation on chemical grouting of inclined fracture to control sand and water flow," *Tunnelling and Underground Space Technology*, vol. 83, pp. 82–90, 2019.

[4] S. Li, R. Liu, Q. Zhang, and X. Zhang, "Protection against water or mud inrush in tunnels by grouting: a review," *Journal of Rock Mechanics and Geotechnical Engineering*, vol. 8, no. 5, pp. 753–766, 2016.

[5] Z. Zhou, X. Cai, X. Du, S. Wang, D. Ma, and H. Zang, "Strength and filtration stability of cement grouts in porous media," *Tunnelling and Underground Space Technology*, vol. 89, pp. 1–9, 2019.

[6] Q. Wang, S. Wang, S. W. Sloan, D. Sheng, and R. Pakzad, "Experimental investigation of pressure grouting in sand," *Soils and Foundations*, vol. 56, no. 2, pp. 161–173, 2016.

[7] Y. Gao and W. H. Sui, "Modelling of chemical grout column permeated by water in transparent soil," *International Journal of Environment and Pollution*, vol. 59, no. 2/3/4, pp. 142–154, 2016.

[8] M. Hyodo, Y. Wu, N. Aramaki, and Y. Nakata, "Undrained monotonic and cyclic shear response and particle crushing of silica sand at low and high pressures," *Canadian Geotechnical Journal*, vol. 54, no. 2, pp. 207–218, 2017.

[9] Y. Wu, H. Yamamoto, J. Cui et al., "Influence of load mode on particle crushing characteristics of silica sand at high stresses," *International Journal of Geomechanics-ASCE*, vol. 20, no. 3, Article ID 04019194, 2020.

[10] S. Wang, X. Lei, Q. Meng, J. Xu, M. Wang, and W. Guo, "Model tests of single pile vertical cyclic loading in calcareous sand," *Marine Georesources & Geotechnology*, pp. 1–12, 2020.

[11] Z. Saada, J. Canou, L. Dormieux, J. C. Dupla, and S. Maghous, "Modelling of cement suspension flow in granular porous media," *International Journal for Numerical and Analytical Methods in Geomechanics*, vol. 29, no. 7, pp. 691–711, 2005.

[12] J. Yoon and C. S. El Mohtar, "A filtration model for evaluating maximum penetration distance of bentonite grout through granular soils," *Computers and Geotechnics*, vol. 65, pp. 291–301, 2015.

[13] M. Axelsson, G. Gustafson, and Å. Fransson, "Stop mechanism for cementitious grouts at different water-to-cement ratios," *Tunnelling and Underground Space Technology*, vol. 24, no. 4, pp. 390–397, 2009.

[14] L. Zhang, *Study on Penetration and Reinforcement Mechanism of Grouting in Sand Layer Disclosed by Subway Tunnel and its Application*, Shandong University, Jinan, China, 2017.

[15] J.-S. Kim, I.-M. Lee, J.-H. Jang, and H. Choi, "Groutability of cement-based grout with consideration of viscosity and filtration phenomenon," *International Journal for Numerical and Analytical Methods in Geomechanics*, vol. 33, no. 16, pp. 1771–1797, 2009.

[16] A. Bezuijen, R. te Grotenhuis, A. F. van Tol, J. W. Bosch, and J. K. Haasnoot, "Analytical model for fracture grouting in sand," *Journal of Geotechnical and Geoenvironmental Engineering*, vol. 137, no. 6, pp. 611–620, 2011.

[17] S. Li, J. Yang, and P. Zhang, "Water-cement-density ratio law for the 28-day compressive strength prediction of cement-based materials," *Advances in Materials Science and Engineering*, vol. 2020, Article ID 7302173, 8 pages, 2020.

[18] P. Yang, Y. Tang, Z. Peng et al., "Study on grouting simulating experiment in sandy gravels," *Chinese Journal of Geotechnical Engineering*, vol. 28, no. 12, pp. 2134–2138, 2006.
[19] Z. Qian, Z. Jiang, L. Cao et al., "Experiment study of penetration grouting model for weakly cemented porous media," *Rock and Soil Mechanics*, vol. 34, no. 1, pp. 139–143, 2013.
[20] L. Zhang, R. Liu, Q. Zhang et al., "Calculation of reinforcement effect of fracture-compaction grouting in soft strata," *Chinese Journal of Rock Mechanics and Engineering*, vol. 37, no. 5, pp. 1169–1184, 2018.
[21] G. Li, *Advanced Soil Mechanics*, Tsinghua University Press, Beijing, China, 2004.